American Journal of Chemistry and Pharmacy (AJCP)

ISSN: 2834-0116 (ONLINE)

VOLUME 5 ISSUE 1 (2026)

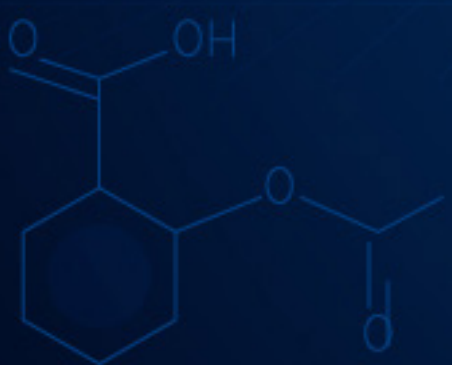

PUBLISHED BY
E-PALLI PUBLISHERS, DELAWARE, USA

American Journal of Chemistry and Pharmacy (AJCP)

Volume 5 Issue 1, Year 2026
ISSN: 2834-0116 (Online)
DOI: https://doi.org/10.54536/ajcp.v5i1.7007
https://journals.e-palli.com/home/index.php/ajcp

Pyro-processed Coconut Fibre for Removal of Lead Ions from Aqueous Solution

Titus M. Kasimu[1*], Francis M. Maingi[2], Harun M. Mbuvi[3], Margaret M. Ng'ang'a[3], Adamu Abdulhameed[4]

Article Information

Received: November 05, 2025
Accepted: February 12, 2026
Published: May 25, 2026

Keywords

Activated Coconut Fibre Charcoal, Adsorbent, Coconut Fibre Charcoal And Lead

ABSTRACT

Approximately 80% of the population in developing countries lacks access to clean, safe water. A major source of water contamination is heavy metal ions, which pose great risks to human health. This is expected to increase with the projected population and industrial growth if immediate remediation is not taken. Current operational methods for removing the heavy metal ions in wastewater include: chemical coagulation, ion exchange, electrochemical methods, adsorption using activated carbon, natural zeolite, membrane process, ultra-filtration, among others, which are uneconomical due to high costs and unaffordable to low-income earners. Coconut fibres are locally available agricultural waste that can be converted by activation into adsorbents for water remediation due to their fineness and large surface area. This study reports the synthesis and characterization of coconut fibre charcoal (CFC) and activated coconut fibre charcoal (ACFC) to remediate water contaminated with Pb^{2+} ions. This involved burning dry coconut fibre in a limited amount of air to obtain coconut fibre charcoal followed by dissolving fine powder of charcoal in 2 M phosphoric acid for 24 hours at a temperature of 25 ºC to obtain activated coconut fibre charcoal. The adsorbents were characterized using FT-IR and SEM. Batch sorption studies were carried out while varying parameters of contact time, shaking speed, temperature, adsorbent dose, pH, and initial concentration of metal ions in solution. Residue Pb^{2+} ion concentrations were determined using atomic absorption spectroscopy (AAS). The FT-IR results showed absorption peaks at 1423 cm^{-1} and 840 cm^{-1} attributed to symmetric –COO- stretch and -OH deformation in ACFC adsorbent, these peaks shifted to 1384 cm^{-1} and 813 cm^{-1} while PO4- aromatic strain vibration in ACFC disappeared upon saturation of ACFC with Pb^{2+} ions respectively. SEM analysis showed pores of different sizes and shapes in ACFC compared to a rigid, concrete, and smooth surface upon saturation with Pb^{2+} ions. Adsorption data for Pb^{2+} ions best fitted into the Freundlich model with maximum adsorption capacities of 32.09 mg lead/g activated coconut fibre charcoal. The results from this study suggest that coconut fibre charcoal and activated coconut fibre charcoal are potential adsorbents of Pb^{2+}ions.

INTRODUCTON

The water quality in developing countries continues to deteriorate due to pressure from inorganic and organic pollutants leaving out a large population of the world with no access to enough safe and clean drinking water (Feng *et al.*, 2021; Peng & Bartzas, 2021). This water scarcity situation is bound to become more problematic in the near future due to the projected global population growth, and increasing micro-pollutant contamination in flora, fauna, air, soil, and water (Peng & Bartzas, 2021). This is accompanied by inadequate water supply infrastructure and high inflation rates, which have hindered the poor's access to clean water in many developing countries. Heavy metal is a (metal or metalloid) element that causes environmental pollution, it is toxic at low concentrations (such as Pb and Hg), or is harmful to organisms at high concentrations (such as Cu and Mo) (Qasem *et al.*, 2021). There has been remarkable growth in light and informal (Jua kali) industries like textiles, leather, paper, plastics, electroplating, cement, metal processing, wood preservatives, paints, pigments, and steel fabricating industries. These industries discharge large quantities of poisonous wastes into water bodies, making water unhealthy for domestic use (Long *et al.*, 2021).

Lead is a non-essential element and poisonous even at very low concentration levels of exposure resulting in impairment of the nervous system and its effect on foetuses, infants, and young children, ischemic heart disease, testicular atrophy, anaemia, and interstitial nephritis (Krauklis *et al.*, 2018). Furthermore, the International Agency for Research on Cancer (IARC) classifies lead as a probable human carcinogen at concentrations above 10 µg/dL. (Kumar *et al.*, 2020). Several processes used to remove dissolved heavy metals include ion exchange, precipitation, ultrafiltration, reverse osmosis, electro-dialysis filtration, and sedimentation which are not cost-effective but are not effective for concentrated ions and produce a lot of sludge (Feng *et al.*, 2021). Ion selectivity is high in ion exchange treatment, but the cost of the resins is too high (Bashir *et al.*, 2019). Coconut fibres are agricultural waste available in large quantities throughout tropical countries. In Kenya, they are found along the coastal region, currently burning is the only way of disposal which contributes significantly to CO2 and methane emissions which are pollutants to the environment. When allowed to settle in water ponds

[1] Department of Physical Sciences, Machakos University, Kenya
[2] Department of Science Technology and Engineering, Kibabii University Bungoma, Kenya
[3] Department of Chemistry, Kenyatta University Nairobi, Kenya
[4] Chemistry Department, Sa'adu Zungur University, Bauchi State, Nigeria
[*] Corresponding author's e-mail: tituskasimu8@gmail.com

they became breeding places for mosquitoes. Due to economic and environmental problems, efforts should be directed toward the utilization, storage, and disposal of coconut fibres. Activated coconut fibre charcoal contains silicate and phosphate groups that can bind metal ions but limited literature is available on the use of coconut shell in waste water treatment despite having large surface area. This study will provide knowledge on coconut shell fibre charcoal and activated coconut shell fibre charcoal towards the removal of lead ions from aqueous solution.

MATERIALS AND METHODS

Reagents and chemicals

Coconut fibre were obtained from Kongowea market, Mombasa County, and transported to Kenyatta University Chemistry laboratories. The coconut fibre was air-dried for three weeks at room temperature (298K) until constant weight was obtained. All the chemicals used were of analytical grade and were used as purchased: Lead (II) nitrate, nitric acid, and phosphoric acid from Kenya Science Chemical Limited, Kenya.

Coconut Fibre Charcoal (CFC)

Fibres from coconut shells were removed from fully mature nuts and then air-dried until constant weight was obtained. The fibres were placed into a 10 litre aluminium cylinder, and heated to expel air and water vapour. The cylinder was then closed and further heated from the bottom. After heating for 12 hours, the content was left to cool and the carbonised product inspected visually to determine fully carbonized fibres. Fibres that retained the brown colour were removed and kept for the next batch of carbonization. Carbonized fibres were coded as CFC.

Activated Coconut Fibre Charcoal (ACFC)

The procedure for activating the charcoal was adopted from Titus *et al.* (2022). The CFC was crushed and ground into powder using a Sheller machine (Honda ESB 501). About 200 g of the grinded sample was weighed and placed in a 1 L Erlenmeyer flask. 500 mL of 2 M solution of phosphoric acid was then added. The mixture was swirled and then allowed to stand for 24 hours at a temperature of 25 ºC for activation to take place. Phosphoric acid introduces phosphate, pyrophosphate, metaphosphate and phenyl phosphate functional groups on the surface of carbon materials making it porous and facilitates binding sites with metal cations (Khanna *et al.*, 2018). The mixture was filtered and the residue was washed with deionized water to remove the excess acid. The residue was air-dried until a constant weight was attained and then coded as ACFC.

Preparation of standard and test solution of Pb^{2+} ions

The stock solution of Pb^{2+} containing 1000 mg/L was prepared by dissolving 1.599 g of lead (II) nitrate in 200 mL of distilled water and diluting to one litre. Serial dilutions were then done to obtain working solutions. A solution of 0.1 M nitric acid and 0.1 M sodium hydroxide was used throughout the experiments to adjust the pH of the solution.

Instrumentation

An atomic absorption spectrophotometer (model AAS 4141 ECIL India) was used to determine levels of Pb^{2+} ions in solutions at wavelength of 283.3 nm. The pH meter (model PHEP Hanna), instrument, was used in this study to determine pH. FT-IR (model Perkin Elmer 100, Waltham Ma; USA) was used for analysis of the functional groups in the adsorbents. SEM (ZEISS SUPRA 60 German) was used to determine the morphology of the adsorbents.

Batch experiments

The parameters under the study were initial metal ions concentration, adsorbent dosage, pH, shaking speed, temperature and contact time. The quantity of Pb^{2+} ions adsorbed per unit mass of the adsorbents and their percentage removal were evaluated using equations 1 and

$$q_e = \frac{(Co-Ce)}{m} V \quad \ldots\ldots\ldots\ldots\ldots 1$$

$$R = 100 \left(\frac{Co-Ce}{Co}\right) \ldots\ldots\ldots\ldots\ldots 2$$

2 respectively;

Where, R= percentage removal
q_e = Amount of metal ion removed per unit mass of adsorbent at equilibrium
C_o = Initial concentration of sorbate
C_e = Concentration of sorbate at equilibrium
m = mass of adsorbent used in grams
V = volume of solution used in litres

The percentage removal of adsorbate was calculated as the ratio of the difference in adsorbate concentration before and after adsorption (Co–Ce) to the initial concentration of the adsorbate of the aqueous solution expressed as a percentage. The optimum values were determined by taking the highest percentage amount of metal ions adsorbed per unit mass of the adsorbent for each batch experiment.

Characterization of the adsorbents

(FT-IR) analysis of the adsorbents

The functional group analysis of the CFC, ACFC and ACFC saturated with Pb2+ ions was done using FT-IR (Shimadzu IR Tracer-100). The samples of the adsorbents were dried at a temperature of 305 K in an oven for 6 hours. The dried sample of each was mixed with pre-dried KBr in a ratio of 25: 1. The fine homogenous mixture was compressed to form a transparent pellet and then analysed using the transmission method at 4000-200 cm^{-1} wavelength range (Hammond *et al.*, 2005).

Microstructural analysis of the adsorbents

The microstructures of the CFC ACFC and ACFC saturated with Pb2+ ions were determined using SEM (ZEISS SUPRA 60 German) bright microscope at an accelerating voltage of 250 kV. The prepared samples were dried in the oven at 45 °C for 6 hours and then coated with gold for analysis (Zhu *et al.*, 2017).

Adsorption Parameters

Effect of initial pH on the Adsorption of Pb^{2+} Ions

The effect of initial pH on the percentage removal of Pb^{2+} ions was done using 1 g of CFC and ACFC. The pH of the solutions was varied from pH 2 to pH 10. At each pH, 1.0 g of the adsorbents were stirred with 50 mL of aqueous metal solutions containing 100 mg/L Pb^{2+} ions solutions at a shaking speed of 120 rpm for 3 hours. At the end of the contact time, samples were centrifuged and concentrations of Pb^{2+} ions were determined using flame atomic adsorption spectrometry.

Effect of Adsorbent Dosage on the Adsorption of Pb^{2+} Ions

The effect of adsorbent doses on the percentage removal of Pb^{2+} ions was investigated by shaking 50 mL of 100 mg/L with varying doses of ACFC, and CFC adsorbents from 0.1 to 2.0 g. The initial pH of the metal ion solutions was adjusted to their respective optimum pH of 6 using nitric acid and sodium hydroxide solutions. The experiments were conducted in triplicate and stirred for 3 hours in plastic bottles of 120 mL on a water bath shaker at 120 rpm. At the end of the contact time, the samples were centrifuged and the concentrations of Pb^{2+} ions were determined using flame atomic adsorption spectrometry.

Effect of Contact Time on the Adsorption of Pb^{2+} Ions

The percentage of Pb^{2+} ions adsorbed at various contact times of 30, 60 90, 120, 150, and 180 minutes was investigated using 50 mL of 100 mg/L sample solutions in 120 mL plastic bottles. 1.0 g ACFC and CFC were added to each bottle. The pH of the sample solutions was adjusted using 0.1 M nitric acid and 0.1 M sodium hydroxide solutions to a required pH of 6. The bottles were stirred on a water bath shaker at 120 rpm. The solutions were then centrifuged and the filtrates were subjected to atomic absorption spectroscopy to record the absorbance of Pb^{2+} ions.

Effect of Initial Concentration on the Adsorption of Pb^{2+} Ions

The effect of the initial concentration of Pb^{2+} ions on the percentage adsorbed was investigated by agitating 50 mL samples of Pb^{2+} solutions of 50, 100, 150, 200, and 250 mg/L in 120 mL plastic bottles with 1.0 g ACFC and CFC adsorbents in a water bath shaker at 120 rpm. The contact time was kept at 2 hours and the initial pH 6 of the test solution was set using 0.1 M of sodium hydroxide and nitric acid, respectively. Samples are removed from the bath shaker after 2 hours and then centrifuged. Concentrations of Pb^{2+} ions were determined using flame atomic adsorption spectroscopy (FAAS). All runs were conducted in triplicates.

Effect of Temperature Changes on the Adsorption of Pb^{2+} Ions

The effect of temperature on Pb^{2+} ions on the percentage adsorbed was investigated by agitating 50 mL samples of Pb^{2+} in 120 mL plastic bottles with 1.0 g of ACFC and CFC adsorbents with varying water bath shaker temperatures of 293 K, 313 K, 333 K, 353 K, and 373 K. The contact time was kept at 2 hours and the initial pH of the test solution was set at pH 6 using 0.1 molar sodium hydroxide and 0.1 molar nitric acid. Samples were withdrawn after 2 hours and then centrifuged. Concentrations of Pb^{2+} ions were determined using FAAS. All runs were conducted in triplicates.

RESULTS AND DISCUSSION

FT-IR analysis of the CFC, ACFC and ACFC saturated with lead

FT-IR analysis was carried out to identify the functional groups present in the adsorbents as well as groups involved in metal ion binding. Figure 1 shows the IR

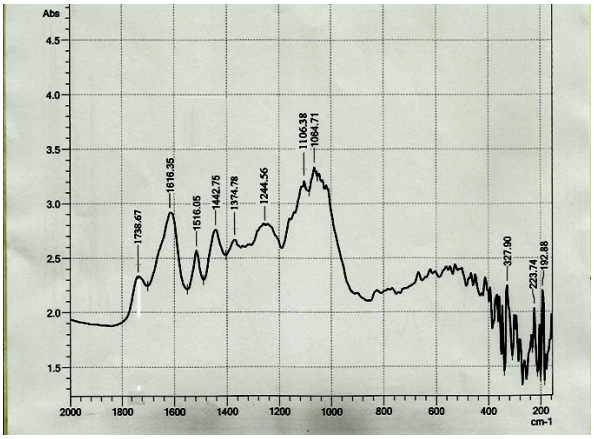

Figure 1: FT-IR spectrum of CFC

spectrum of CFC.

The absorption peaks at around 1738.67 cm^{-1} are accredited to the stretching vibration of C=O in non-conjugated esters, carbonyls, and ketones. 1616.35 cm^{-1} is the relative pure ring stretching mode associated with aromatic -C-O–CH_3, C=C aromatic ring stretching mode is assigned to 1516.05 cm^{-1}. The broad band at 1442.75 and 1374.78cm^{-1} are caused by -CH2 scissors and -O-CH in stretching vibration. 1244.56 cm^{-1}, was due to -O-H phenolic, 1106.38cm-1 was assigned to -O-H in alcohol and ether in vibration mode while 1064.71 cm^{-1} was from aromatic C- H in-plane bending deformation (Wanga *et al.*, 2016; Luo *et al.*, 2018).

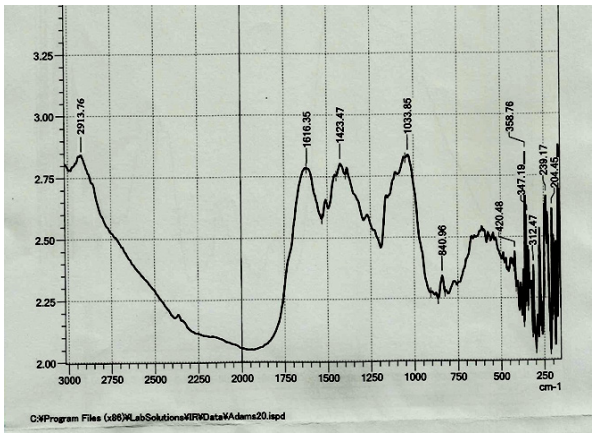

Figure 2: FT-IR spectrum of activated coconut fibre charcoal, (ACFC)

Figure 2 shows the FT-IR spectrum of phosphoric activated coconut fibre charcoal. As shown, new peaks are observed at 2913 cm^{-1}, 840 cm^{-1} and 1423 cm^{-1} associated with -CH_3 in lignin, -OH deformation vibration and symmetric -COO-stretching bands as compared with Figure 1 (Wanga *et al.*, 2016). On the other hand a broad peak at 1033 cm^{-1}.associated with strain vibration of ionized P+O- upon activation (Khanna *et al.*, 2018; Singh & Kaur, 2013). This shows that CFC was successfully activated to ACFC. Figure 3 shows the FT-IR spectrum of ACFC saturated with Pb^{2+} ions.

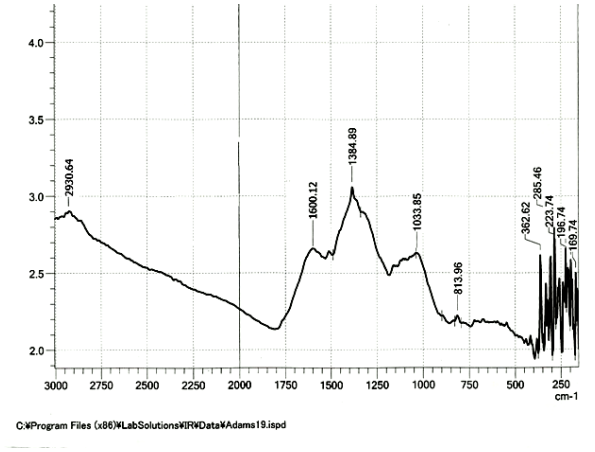

Figure 3: FT-IR spectrum of activated coconut fibre charcoal (ACFC) saturated with Pb^{2+} ions

The spectrum showed significant shifts in some absorption peaks when compared with Figure 2. The -COO- symmetric vibration peak at 1423 (Figure 2) shifted to 1384 cm^{-1} in addition to a new peak at 1600 cm^{-1} assigned to -COO- asymmetric vibration. Further, the small peak at 840 cm^{-1} (Figure 2) associated with -OH deformation shifted to 813 cm^{-1} while a peak at 1033 cm^{-1} (Figure 2) disappeared on saturation of ACFC with Pb^{2+} ions. This shows that -COO-, PO_4- and -OH functional groups are involved in binding Pb^{2+} ions. Similar results have been reported by Banerjee *et al.* (2014).

Scanning electron microscope (SEM) of CFC, ACFC and ACFC saturated with lead

SEM images were used to analyse the morphological structure of the adsorbents. The SEM images of the CFC, ACFC and ACFC saturated with Pb^{2+} ions adsorptions are presented in Figure 4.

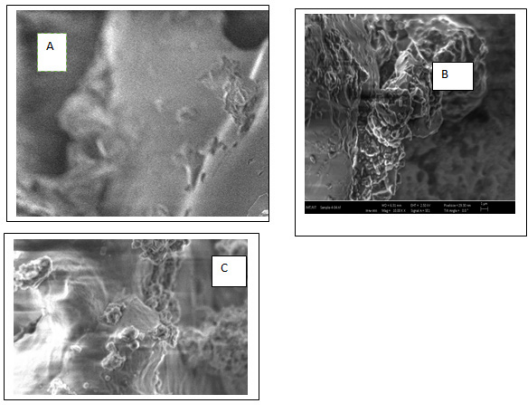

Figure 4: SEM micrographs of the (A) CFC, (B) ACFC and (C) ACFC saturated with Pb^{2+} ions

From the micrographs in Figure 4, it is clear that CFC is an amorphous and rigid structure without voids and pores on its surface (Figure 4A). This shows the complete carbonization of coconut fibre to charcoal (Titus *et al.*, 2022). However, after activation with phosphoric acid, ACFC showed surface modification that was different from that of CFC. A well-developed microporous structure with smooth irregular pores and lamina structural nature occurred on the surface of the powdered ACFC Figure 4(B). Upon saturation with Pb^{2+} ions, a rigid structure with no pores was formed. This could be attributed to the fact that the pores in ACFC were occupied by the metal ions.

The Effect of pH on Pb^{2+} Ions Percentage Removal

Figure 5 shows the effects of pH on the percentage removal of Pb^{2+} ions. The pH was varied from 2 to 10 using ACFC and CFC as adsorbents.

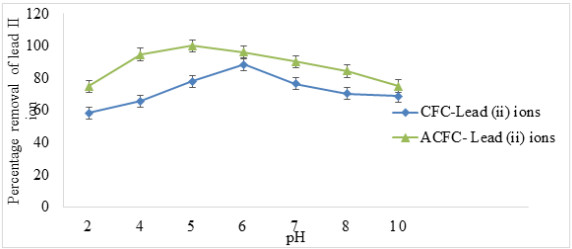

Figure 5: Effect of pH on Pb^{2+} ions percentage removal (adsorbent dose= 1.0 g, contact time =180 minutes, shaking speed= 120 rpm, temperature= 298 K and working solution =50 mg/L of Pb^{2+} ions).

Figure 5 shows that there was progressive increase for the percentage removal of Pb^{2+} ions by CFC and ACFC from 58.31% to 88.52.1% and 74.95% to 99.96% as pH changes from 2 to 6 and 2 to 5 respectively. However, percentage removal decreased to 68.8% in CFC and 75.01 % in ACFC as the pH value increased from 7 to 10 and 6 to 10 respectively. The results show that lower pH values are associated with a high rate of adsorbent surface protonation of the active sites, preventing the adsorption of Pb^{2+} ions by the adsorbent (Zahid Mahmood *et al.*, 2017). The increased adsorption is due to an increased number of vacant sites as linked H+ ions are released from the adsorbate facilitating a high rate of Pb^{2+} ions adsorption (Habid, 2017). However, the formation of soluble metal hydroxyl complexes decreased the rate of adsorption as pH values increased above 7 Therefore adsorption experiments for Pb^{2+} ions are better executed at moderate pH between 5 and 6.

Effect of Contact Time on Adsorption Process of Pb^{2+} Ions

Figure 6 investigates the effect of contact time on adsorption of Pb^{2+} ions by CFC and ACFC. Adsorption residence time was varied from 30 to 180 minutes.

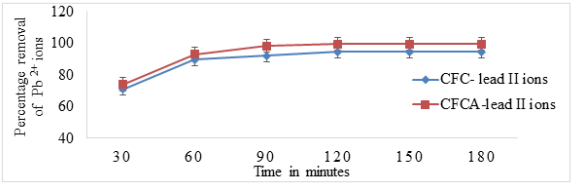

Figure 6: The effect of contact time on Pb^{2+} ions percentage removal (adsorbent dose =1.0 g, pH=6, shaking speed =120 rpm, temperature= 298 K and working solution= 50 mg/L of Pb^{2+} ions)

From Figure 6, the percentage of adsorbed Pb^{2+} ions by CFC and ACFC increased from 70.89 % to 94.6 % and 74.05 % to 99.6%, respectively as time was adjusted from 30 to 120 minutes, followed by plateau in adsorption. The progressive increase in adsorption was associated with the initial high concentration gradient between the adsorbate in solution and the high number of vacant sites present on the surface at the beginning (Petrella *et al.*, 2018). On the other hand, as contact time increases the concentration of metal ions in solution decreases as the vacant surface sites become saturated. The rate of adsorption equates to the rate of desorption attaining equilibrium in the percentage of Pb^{2+} ions removal from the solution (Jeyakumar & Chandrasekaran, 2014).

The Effect of Adsorbent Dosage in Pb^{2+} Ions Percentage Removal

Figure 7 shows the effect of the adsorbent dose of CFC and ACFC on adsorption of Pb^{2+} ions percentage removed by CFC and ACFC as adsorbents amounts were varied from 0.1 g to 2.0 g while keeping all other conditions and parameters the same.

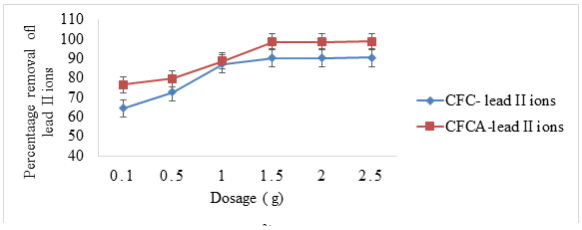

Figure 7: The effect of adsorbent dosage on Pb^{2+} ions percentage removal (Contact time=180 minutes, pH= 6, shaking speed=120 rpm, initial metal ion concentration=50 mg/L and temperature=298 K).

Figure 7 indicates that as the adsorbent dose increased, the percentage removal of Pb^{2+} ions increased from 76.54 % to 98.64 % and from 64.3 % to 90.26 % when the dosage of CFC and ACFC was increased from 0.1 g to 1.5 g, respectively This is due to the more readiness of the exchangeable vacant sites or surface area at higher concentration of the adsorbent (Edris *et al.*, 2012). However, adsorptions become constant due to the shielding effect on vacant sites as a result of the screening effect on the dense outer layer of the cells at higher concentrations of dosage (Ahmed *et al.*, 2023).

The effect of shaking speed on Pb^{2+} ions percentage removal

Figure 8 shows the effect of the shaking speed on the percentage of Pb^{2+} ions removed by CFC and ACFC when the shaking speed was varied from 20 to 120 revolutions per minute (rpm) while keeping all other conditions and parameters the same.

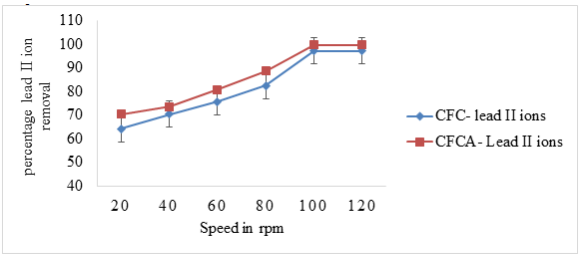

Figure 8: The effect of shaking speed on Pb^{2+} ions percentage removal (adsorbent dose=1.0 g, contact time= 180 minutes, pH= 6, temperature=298 K and initial metal ion concentration=50 mg/L).

Figure 8 shows a gradual increase in the percentage removal of Pb^{2+} ions with increasing shaking speed. The percentage removal of Pb^{2+} ions by CFC and ACFC increased from 64.13 % to 97.21 % and from 70.27 to 99.65 % as shaking speed increased from 20 to 100 rpm

respectively. However, there was no significant change in the percentage removal of Pb^{2+} ions for shaking speed values of adsorbents above 100 rpm. This indicates that an increase in shaking speed enhances the diffusion of metal ions towards the surface of the adsorbent due to increased kinetic energy which breaks forces between the Pb2+ ions in solution and the binding sites which are made readily available promoting a fast rate of transfer of sorbate ions to the sorbent sites (Argun *et al.*, 2007). Shaking speed should be enough to ensure cell surfaces for binding sites are available for the adsorption process to occur, shaking speed of 120 rpm was selected as the optimum speed for Pb^{2+} ions.

Effect of Temperature Changes on Adsorption of Pb^{2+} Ions

Figure 9 shows the effect of the temperature change on the adsorption of Pb^{2+} ions using CFC and ACFC adsorbents. Temperatures was varied from 273 K to 373 K.

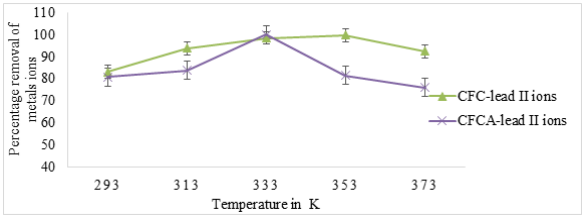

Figure 9: The effect of temperature on Pb^{2+} ions percentage removal (adsorbent dose=1.0 g, contact time= 180 minutes, pH= 6, shaking speed=120 rpm and initial metal ion concentration= 50 mg/L).

Figure 9 indicates that the percentage removal of Pb^{2+} ions using CFC at 298 K increased gradually from 83.07 to 99.60 % at 353 K followed by a decrease to 92.43 % at 373 K. on the other hand the percentage removal of Pb^{2+} ions using ACFC increased from 80.68 to 99.86 % as temperature increased from 293 to 333 K followed by a decrease to 76.02 % as temperature increased to 373 K. The above trends show that increasing temperature increases the kinetic energies of ions and opens up extra sorption sites in the adsorbents increasing their adsorption capacities but for temperature above 333 K electrostatic force of attraction between binding sites and adsorbate decreases favouring the rate of desorption leading to decreased Pb^{2+} ions removal (Nleonu *et al.*, 2023).

Effect of Initial Metal Ions Concentration on the Adsorption of Pb^{2+} Ions

The effect of metal ions concentrations on percentage removal of Pb^{2+} ions using CFC and ACFC. The results obtained upon varying the initial metal ions concentration from 50 to 250 mg/L for Pb^{2+} ions is summarized in Table 1.

The mean Percentage removal of Pb^{2+} ions in CFC

Table 1: The effect of initial concentration of Pb^{2+} ions percentage removal

	Amount of Pb2+ adsorbed by CFC	Amount of Pb2+ adsorbed by ACFC
Initial concentration in mg /L	**Mean ± SE**	**Mean ± SE**
50	76.68±1.66	81.67±0.22
100	85.07±1.78	94.54±0.23
150	93.30±1.82	99.68±0.21
200	82.34±1.88	86.93±0.23
250	71.43±1.99	84.41±0.22

(Adsorbent dose=1.0 g, pH= 6, contact time= 180 minute, shaking speed=120 rpm, temperature=298 K and initial metal ion concentration=50 mg/L)

increased rapidly from 76.68 % to 93.30 % as the initial concentration increased from 50 mg/L to 150 mg/L, followed by a decrease to 71.43 % at a concentration of 250 mg/L (Table 1). Again, on using ACFC mean percentage removal of Pb^{2+} ions increased from 81.67 % to 99.86 % as the initial concentration increased from 50 mg/L to 150 mg/L, followed by a decrease to 84.4 % at a concentration of 250 mg/L. As the initial concentration increases from 50 to 150 mg/L rate of percentage removal is very high due to the presence of active and large surface area of vacant sites in the adsorbent. This provides increased dynamic force to overcome all mass transfer resistance of metal ions between the aqueous and solid phases, resulting in a higher possibility of collision between metal ions and sorbents (Mureithi *et al.*, 2012). The low adsorption capacity at higher concentrations is due to a smaller number of binding sites on the adsorbent surface compared to more number of adsorbing species (Meez *et al.*, 2021; Senthil *et al.*, 2010).

Adsorption Isotherms

In this study, Langmuir and Freundlich adsorption isotherms were used to demonstrate the relationship between the amounts of Pb^{+2} ions adsorbed at their equilibrium concentrations in solution. The analysis of the adsorption data by fitting it into the isotherm models is a crucial step for finding a suitable model to be used for a design purpose (Renu *et al.*, 2017). Isotherms parameters constants for CFC and ACFC are summarized in Table 2. Table 2 shows that sorption data for CFC best fit into the Freundlich isotherm model as implied by the R2 = 0.9781 compared to Langmuir's values of 0.5419, respectively. Data for ACFC best fits into the Langmuir isotherm with R^2 = 0.9864, compared to the Freundlich values of 0.5854, respectively. ACFC had the highest affinity for Pb^{2+} ions as implied by the b value of 1.2852 dm^3/g when compared to that for CFC of 0.1271 dm3/g. This indicates that the mobility of Pb^{2+} towards ACFC was high compared to that of CFC used in this study. Despite the Freundlich

model for ACFC, having higher adsorption capacity (Kf) values of 1.0 ×1049 mg/g than corresponding values in the Langmuir model of 1.4306 mg/g the adsorption intensity (1/n) values for the Freundlich model were greater than one hence the adsorption was unfavourable for this model indicating cooperate adsorption process (Pap *et al.*, 2020). CFC fits in the Freundlich model with an adsorption intensity of less than one. 1/n values of < 1 indicate a normal Freundlich adsorption model and Kf can be used to estimate adsorption capacity (Xiao *et al.*, 2017). CFC had the highest adsorption capacity of Kf of 7.7108 mg/g compared to ACFC values of 1.4306 mg/g, respectively.

Table 2 shows that sorption data for CFC best fit into the Freundlich isotherm model as implied by the $R^2 = 0.9781$ compared to Langmuir's values of 0.5419, respectively. Data for ACFC best fits into the Langmuir isotherm with $R^2 = 0.9864$, compared to the Freundlich values of 0.5854, respectively. ACFC had the highest affinity for Pb^{2+} ions as implied by the b value of 1.2852 dm3/g when compared to that for CFC of 0.1271 dm3/g. This indicates that the mobility of Pb2+ towards ACFC was high compared to that of CFC used in this study. Despite the Freundlich model for ACFC, having higher adsorption capacity (Kf) values of 1.0 ×1049 mg/g than corresponding values in the Langmuir model of 1.4306 mg/g the adsorption intensity (1/n) values for the Freundlich model were greater than one hence the adsorption was unfavourable for this model indicating cooperate adsorption process (Pap *et al.*, 2020). CFC fits in the Freundlich model with an adsorption intensity of less than one. 1/n values of < 1 indicate a normal Freundlich adsorption model and Kf can be used to estimate adsorption capacity (Xiao *et al.*, 2017). CFC had the highest adsorption capacity of Kf of 7.7108 mg/g compared to ACFC values of 1.4306 mg/g, respectively.

Table 2: Langmuir and Freundlich parameters for Pb^{2+} ions adsorption by CFC and ACFC

Langmuir				Freundlich		
Adsorbent	**Qmax mg/g**	**b dm^3/g**	**R^2**	**1/n**	**Kf mg/g**	**R^2**
ACFC	1.4306	1.2852	0.9864	14.119	1x1049	0.5854
CFC	0.2070	0.1271	0.5419	0.4671	7.7108	0.9781

CONCLUSIONS

FT-IR spectra show that ACFC contained phosphate, hydroxyl and carboxylate ions on solid support surfaces, which are responsible for Pb^{2+} ions adsorption. SEM analysis suggested a rigid, concrete, and smooth surface in ACFC saturated with lead ions as compared to the uneven surface with the dispersal of a polar phase in ACFC. This showed that activation using phosphoric acid promotes high formation of pores in the carbon. The adsorption capacity of Pb^{2+} ions by CFC and ACFC was optimum at pH 6, adsorbent dosage 1.5 g, initial concentration 150 mg/L, time 180 minutes, temperature 333 K and agitation speed of 120 rpm. The Sorption studies of lead ions by CFC best-fitted the Freundlich isotherm model with a maximum adsorption capacity of 7.7108 mg/g, but the sorption of Pb^{2+} ions by ACFC best-fitted the Langmuir isotherm with an adsorption capacity of 1.4306 mg/g. The study showed that ACFC and CFC are effective adsorbents for the removal of Pb^{2+} ions from aqueous solutions.

Declaration of Interests

The authors declare that they have no known competing financial interests or personal relationships that could appear to have influenced the work described in this paper. No funding was received for conducting this study.

REFERENCES

Ahmed, H.M., Sobhy, N.A., and Hefny, M.M. (2023). Evaluation of agrowaste species for removal of heavy metals from synthetic wastewater. *Journal of Environmental and Public Health,* 1-20.

Argun, M. E., Dursun, S., Ozdemir, C., and Karatas, M. (2007). Heavy metal adsorption by modified oak sawdust: Thermodynamics and kinetics. *Journal of Hazardous Materials,* 141: 77–85.

Banerjee, S., Chattopadhyaya, M., Srivastava, V., Sharma, M. (2014). Adsorption studies of methylene blue onto activated saw dust: kinetics, equilibrium, and thermodynamic studies. *Environmental Progress & Sustainable Energy,* 33: 790-799

Bashir, A., Malik, L., Ahad, S., Manzoor, T., Bhat, M., Dar, G. (2019). *Removal of heavy metal ions from aqueous system by ion-exchange and biosorption methods journal of Environmental chemistry 17:* 729–754.

Edris, G., Alhamed, Y., and Alzahrani, A. (2012). Cadmium and Lead Biosorption by Chlorella Vulgaris. *In Sixteenth International Water Technology Conference (IWTC 16); Istanbul,* Turkey.

Feng, R., Zhao, P., Zhu, Y., Yang, J., Wei, X., Yang, L. (2021). Application of inorganic selenium to reduce accumulation and toxicity of heavy metals (metalloids) in plants: the main mechanisms, concerns, and risks. *Journal of Environmental Science. 771:* 144 - 776.

Habib K (2017). Effect of pH and initial pb (II) concentration on the lead removal efficiency from industrial wastewater using Ca(OH)2. *International Journal of Wastewater Treat,* 3:1–4.

Hammond, P., Ali, D. and Cumming, R. (2005). A system on chip digital pH meter for use in a wireless diagnostic capsule. *Biomedical Engineering, 4:* 687-694.

Jeyakumar, S., and Chandrasekaran, V. (2014). Adsorption of Lead (II) Ions By Activated Carbons Prepared from Marine Green Algae: Equilibrium and Kinetics

Studies. International Journal of Industrial Chemistry, 5: 10.

Khanna, E., Shahjahana, and T. A., (2018). Adsorption of methyl red on activated carbon derived from custard apple (Annona squamosa) fruit shell: equilibrium isotherm and kinetic studies. *Journal of molecular liquid, 249:*1195-1211.

Krauklis, A., Gagani, A., and Echtermeyer, A. (2018). Near infrared spectroscopic method for monitoring water content in epoxy resins and fiber reinforced composite. *Journal of Environmental Chemical Engineering, 11:* 586–599.

Kumar, A., Kumar, A., Cabral-Pinto, M. (2020). Lead toxicity health hazards, influence on food chain, and sustainable remediation approaches. *International Journal of Environmental Research and Public Health, 17*:2179

Long, Z., Huang, Y., Zhang, W (2021) Effect of different indus-trial activities on soil heavy metal pollution, ecological risk, and health risk. *Environmental Monitoring and Assessment 193*:1–12

Luo, X., Li, C., Müller., K., Yu, H., Huang, P., Li, T., sang, T., Bolan, N., Rinklebe J., Wang H. (2018). Sorption of norfloxacin, sulfamerazine and oxytetracycline by KOH-modified biochar under single and ternary systems. *Bioresource Technology, 263:* 385-392.

Meez, E., Rahdar, A., and Kyzas, G. (2021). Sawdust for the Removal of Heavy Metals from Water, journal of Review. *Molecules, 26*(14): 4318.

Mureithi, G., Onindo, O. and Muthakia, G. (2012). Kinetic and equilibrium study for the sorption of Pb (II) ions from aqueous phase by water hyacinth (Eichhorniacrassipes). *Bulletin of the Chemical Society of Ethiopia, 2:* 181-193.

Nleonu, E.C., Onyemenonu, C.C., Okeke, P.I. and Opara, J.N. (2023). Adsorption characteristics of Chrysophyllumalbidum (African Star Apple) peels towards heavy metal ions. *Journal of Chemical Review and Letters, 6:* 44-54.

Pap, S., Kirk, C., Bremner, B., Maja, M., and Taggart, M (2020). Low-cost chitosan-calcite adsorbent development for potential phosphate removal and recovery from wastewater effluent. *Journal of water research, 173:* 115573-115586.

Peng, L., and Bartzas, G. (2021). Editorial overview: heavy metals and metalloids: a serious threat to environment and human health. *Environmental Health Science,* 23: 100287. 2468-5844.

Petrella, A., Spasiano, D., Acquafredda, P., De Vietro, N., Ranieri, E., Cosma, P., Rizzi, V., Petruzzelli, V. and Petruzzelli, D., (2018). Heavy metals Retention Pb(II), Cd(II) from single and multi-metal solution by natural biosorbents from the Olive oil milling operations. *Process Safety and Environment Protection,* 114: 79-90.

Qasem, N., Mohammed, R., and Lawal, D. (2021). Removal of heavy metal ions from wastewater: a comprehensive and critical review. J*ournal of Clean. Water,* 4: 36.

Renu, Agarwal, M., and Singh, K. (2017). *Heavy metal removal from waste-water using various adsorbents, journal of water reuse and desalination, 7*(4): 387–419.

Senthil, K. P., Ramakrishnan, K., Kirupha, S. D., and Sivanesan, S. (2010). Thermodynamic and Kinetic Studies of Cadmium Adsorption from Aqueous Solution onto Rice Husk. *Brazilian Journal of Chemical Engineering,* 27: 347–355.

Singh, J., and Kaur, G. (2013). Freundlich , Langmuir adsorption isotherms and kinetics for the removal of malachite green from aqueous solutions using agricultural waste rice straw. *International Journal of Environmental Sciences,* 4: 250–258.

Titus, M., Harun, M. and Maingi, F.M. (2022). Evaluation of Activated Charcoal Based Hydrogels Functionalized with Maleic Acid on Growth Performance of Zea Mays in Semi-arid Regions of Kenya. *International Journal of Agriculture & Environmental Science, 9*(3), 69-76.

Wang, X., Ren, H., Sun, L., Ma, H., Zhu, J. (2016). Sorption of polychlorinated biphenyls onto bio chars derived from corn straw and the effect of propranolol. *Bio resource Technology,* 219: 458-465.

Xiao, X., Liu, X., Zhang, S., and Zheng, S. (2017). Phosphorus removal and recovery from secondary effluent in sewage treatment plant by magnetite mineral micro particles, *Powder technology,* 306: 68-73.

Zahid, ZM., Athar, A., Uzma, U. (2017). Sorption studies of cadmium ions on alginate-calcium carbonate composite beads. *Journal of Applied Water Science,* 7:915–922.

Zhu, S., Wang, J., Yan, H., Wang, Y., Zhao, Y., Feng, B., Duan, K. and Weng, J. (2017). An injectable supramolecular self-healing bio-hydrogel with high stretch ability, extensibility and ductility, and a high swelling ratio. *Journal of Material Chemistry,* 5: 7021.